




Startup scheme optimization and flow instability of natural circulation lead-cooled fast reactor SNCLFR-100

Wen-Shun Duan¹ · Ze-Ren Zou¹ · Xiao Luo¹ · Hong-Li Chen¹ 

Received: 24 July 2021 / Revised: 18 September 2021 / Accepted: 3 October 2021 / Published online: 26 November 2021
© The Author(s), under exclusive licence to China Science Publishing & Media Ltd. (Science Press), Shanghai Institute of Applied Physics, the Chinese Academy of Sciences, Chinese Nuclear Society 2021

Abstract Owing to the inherent instability of the natural circulation system, flow instability can easily occur during the operation of a natural circulation lead-cooled fast reactor, especially during the startup phase. A comprehensive startup scheme for SNCLFR-100, including primary and secondary circuits, is proposed in this paper. It references existing more mature startup schemes in various reactor types. It additionally considers the restriction conditions on the power increase in other schemes and the characteristics of lead-based coolant. On this basis, the multi-scale coupling code ATHLET-OpenFOAM was used to study the flow instability in the startup phase under different power-step amplitudes and power duration times. The results showed that obvious flow instability phenomena were found in the different startup schemes, such as the short-term backflow phenomenon of the core at the initial time of the startup. Moreover, an obvious increase in the flow rate and temperature to the peak value at the later stage of a continuous power rise was observed, as well as continuous oscillations before reaching a steady state. It was determined that the scheme with smaller power-step amplitude and a longer power duration time requires more time to start the reactor. Nevertheless, it will be more conducive to the safe and stable startup of the reactor.

Keywords Natural circulation · Lead-cooled fast reactor · Startup scheme · Flow instability · Multi-scale coupling

List of symbols

m Mass flow rate (kg/s)
 T Temperature (°C)
 P Pressure (MPa)

1 Introduction

The natural circulation lead-cooled fast reactor has satisfactory passive safety characteristics. However, owing to the lack of a stable driving head provided by a mechanical pump, the precise balance between the driving head and the circuit pressure drop cannot be achieved in the natural circulation system. Wang et al. [1] studied flow oscillation characteristics in a natural circulation system. The use of natural circulation has generated concern regarding operating conditions, especially those relating to the startup phase of the reactor. The two-phase flow instability of the natural circulation boiling water reactor (BWR) was studied at the Indian Institute of Technology [2] during the reactor startup phase. Gesellschaft für Anlagen- und Reaktorsicherheit (GRS) of Germany [3] and the University of Tokyo [4] have studied the startup characteristics of single-phase natural circulating water circuits and observed the phenomenon at the startup stage. Jiang et al. [5] and Chen et al. [6] carried out experimental studies on the startup instability of nuclear reactors, including the unstable phenomenon of the two-phase natural circulation condition.

For the safe operation of a natural circulation lead-cooled fast reactor, it is important to devise an appropriate startup procedure. The startup of a reactor is a complex

✉ Hong-Li Chen
hlchen1@ustc.edu.cn

¹ School of Nuclear Science and Technology, University of Science and Technology of China, Hefei 230027, China

process involving many parameter changes, and there are different startup procedures in accordance with different types of reactors. There are no experimental data to provide a reliable startup scheme for natural circulation lead-cooled fast reactors. However, a suitable scheme for primary and secondary circuits can be developed by referencing more mature schemes for existing reactor types. For existing liquid-metal reactors, the sodium-cooled fast reactor has a relatively mature reactor startup scheme, such as the French superphoenix reactor [7].

For the ALFRED-driven lead-cooled fast reactor, Milan Polytechnic University [8] proposed a startup scheme of a linear power rise based on the startup experience of a sodium-cooled fast reactor. Nonetheless, there remains a lack of startup schemes for natural circulation lead-cooled fast reactors. In 2020, Sun Yat-sen University [9], referencing the startup of some natural circulation systems, proposed a startup scheme for the linear power function and step power function for SNCLFR-100. However, there was a lack of secondary circuit models. Coupling between the primary and the secondary circuits will seriously affect the response process of various parameters of the primary circuit; thus, it is necessary to establish a more comprehensive scheme for the startup, which includes both primary and secondary circuits.

The multi-scale thermo-hydraulic coupling code includes the advantages of the system code and computational fluid dynamics (CFD) code, which can quickly and comprehensively model the various components of the entire reactor loop. In addition, they can capture the locally important three-dimensional phenomena to realize fast and precise numerical simulation of the thermal-hydraulic characteristics of the lead-cooled fast reactor with a pool-type structure and local thermo-hydraulic characteristics. In 2020, the ATHLET system code and the multi-scale coupling code were used to calculate and compare the results, respectively, under the condition of the flow instability caused by a continually changing heating power and mass flow rate on the secondary side of the heat exchanger [10]. Furthermore, the Shanghai Institute of Applied Physics analyzed the thermal-hydraulic characteristics of a molten salt reactor with a coupling scheme between the open-source codes OpenMC and OpenFOAM [11].

In this paper, a comprehensive startup scheme that includes primary and secondary circuits for SNCLFR-100 is proposed. The multi-scale coupling code ATHLET-OpenFOAM developed by GRS [12] was used to study the flow instability phenomenon in the process of selecting the optimal scheme by comparing different startup schemes.

2 Geometry and calculation model

2.1 SNCLFR-100 reactor

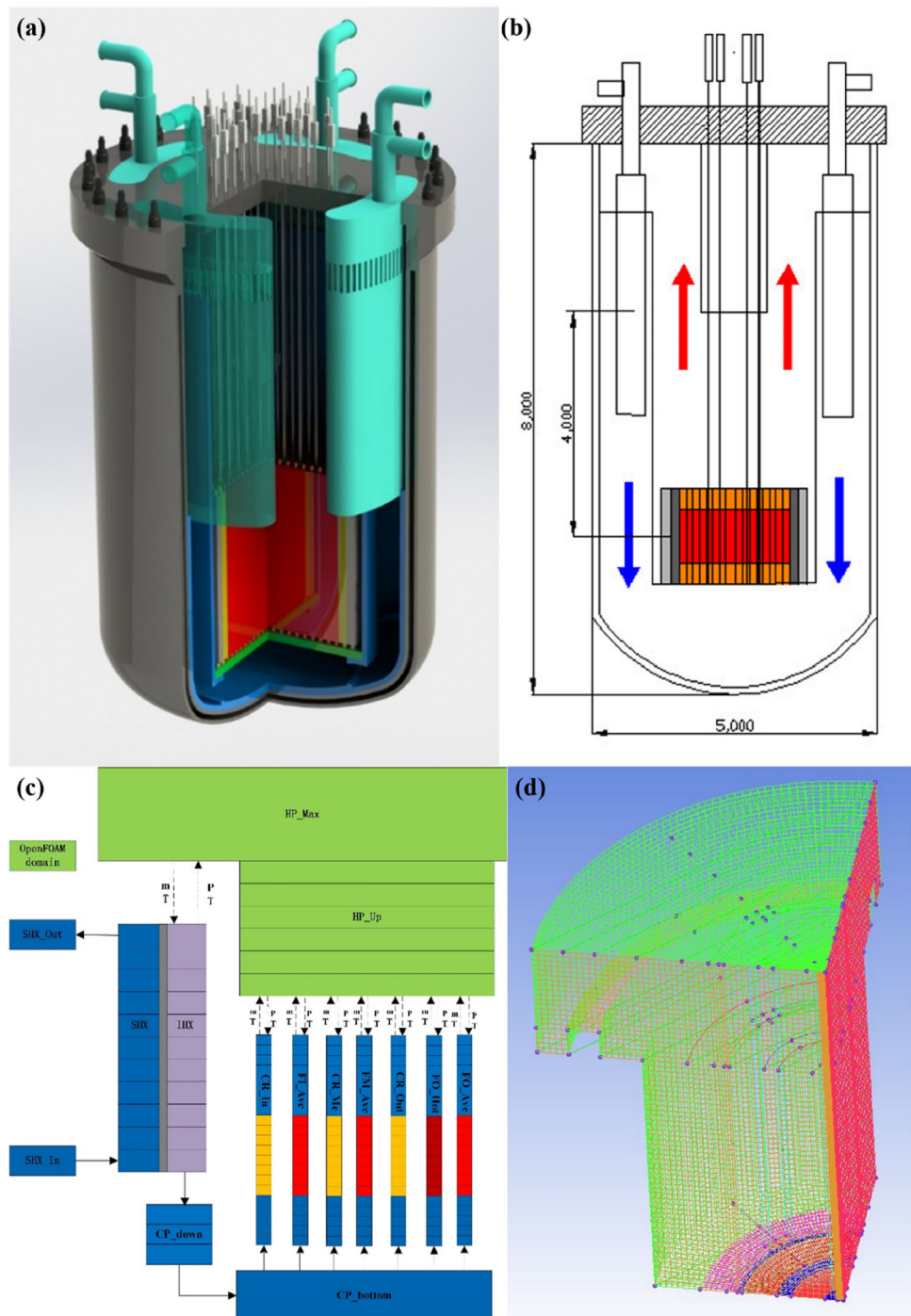
In 2016, the University of Science and Technology of China proposed a small modular natural circulation lead-cooled fast reactor (SNCLFR-100) [13]. A safety analysis of SNCLFR-100 was also carried out [14]. SNCLFR-100 has a design refueling cycle of ten years, a core life of 30 years, and a thermal power of 100 MWth. The primary circuit adopts an integrated pool design with a design height of 4 m of natural circulation. The average temperature of the core inlet coolant was designed to be 400 °C and the average temperature of the outlet coolant is 480 °C. The reactor core adopts a quadrilateral fuel assembly, and it is composed of fuel assemblies, control rod assemblies, safety rod assemblies, reflector layers, and shielding layer assemblies. The fuel consists of mixed oxide (MOX) and the cladding is made of T91. To flatten the power distribution, the core fuel assembly is divided into an inner region (16% $\text{PuO}_2 + 84\%\text{UO}_2$), middle region (19% $\text{PuO}_2 + 81\%\text{UO}_2$), and outer region (24% $\text{PuO}_2 + 76\%\text{UO}_2$). The secondary circuit adopts a water/superheated steam Rankine cycle and the design pressure of the system is 18 MPa. The overall structure design of the SNCLFR-100 is shown in Fig. 1a and b.

2.2 Calculation model

The coupling model of ATHLET-OpenFOAM is shown in Fig. 1c, in which the upper plenum is simulated using OpenFOAM and the rest of the primary and secondary circuits are simulated by ATHLET. The transfer directions of the mass flow rate (m), temperature (T), and pressure (P) are shown in Fig. 1c. The core is divided into seven regions: the inner control rod assembly area (CR_In), inner fuel assembly area (FI_Ave), intermediate control rod assembly area (CR_Me), intermediate fuel assembly area (FM_Ave), external control rod assembly area (CR_Out), external hottest assembly (FO_Hot), and external fuel assembly average area (FO_Ave). The model consists of eight coupling interfaces, seven of which are located at the exits of the seven core regions and the last interface at the inlet of the heat exchanger. Owing to the symmetry of the reactor, only a quarter of the entire reactor model was built to simplify the calculation.

As shown in Fig. 1d, the inlet of the upper plenum area simulated by OpenFOAM corresponds to the outlet of the corresponding seven core areas, in which the outlet area of the inner control rod assembly area of the core is equivalent to a circle at the same position and the outlet area of the hottest fuel assembly in the core is equivalent to a

Fig. 1 (Color online) The structure and coupling model of SNCLFR-100



quadrilateral. The remaining core exit area is equivalent to the corresponding area of the annular region at the same location. The boundary conditions of the left and right surfaces are symmetric, while the remaining surfaces are wall boundaries; that is, they are all assumed to be adiabatic and non-slip conditions.

3 Study of startup scheme of natural circulation lead-cooled fast reactor

3.1 Confirmation of reactor primary circuit startup scheme

A suitable startup scheme for natural circulation lead-cooled fast reactors can currently be established by referencing the more mature schemes of pressurized water

reactors (PWRs), natural circulation boiling water reactors, and sodium-cooled fast reactors. In addition, some special physical and chemical properties of the coolant lead should be considered in the power-up scheme. (1) Lead has a stronger thermal conductivity than water and its boiling point is 1740 °C at atmospheric pressure. Therefore, it is not necessary to consider that a too rapid power rise will lead to the vaporization of the coolant and the formation of a boiling crisis on the surface of the cladding. (2) Compared with the PWR, BWR, and supercritical water reactor (SWR), the system operating pressure of the lead-cooled fast reactor is at an atmospheric pressure of 0.1 MPa. Moreover, there is no sudden change in thermal conductivity and in the two-phase flow instability caused by sudden changes in pressure.

Owing to the high boiling point and high thermal conductivity of the coolant lead, the power-step amplitude of the lead-cooled fast reactor can be larger and the power duration time can be shorter than that of the PWR in the startup phase. Therefore, the designed power-step amplitude is 10%, which is the same as that of the sodium-cooled fast reactor and the power duration time is 2 min.

For the natural circulation reactor, there is still a large degree of natural circulation in the reactor after the hot shutdown and the mass flow rate remains at a high level. The cold startup of the reactor refers to the process of power starting from zero to full power and the mass flow rate in the reactor is zero at the initial moment of the cold startup. To study the possible backflow and flow oscillation in the startup phase, a cold startup is selected as the research object. To simplify the calculation process, it is assumed that some physical tests and other tests in the startup phase have been completed and the startup time occupied by the test is small compared with the power rise time. In other words, it is assumed that the startup time occupied by the test is not considered in the startup process.

The initial and transient conditions of the SNCLFR-100 are as follows: (1) Initially, the temperature of the coolant lead of the primary circuit is 380 °C, the total mass flow rate of the primary circuit is 0 kg/s, the system pressure is 0.1 MPa, and the initial power is 0 W. (2) The power starts from 0 s and gradually increases to full power as a step function. (3) At the initial time, the mass flow rate of the inlet of the secondary side of the main heat exchanger is 0 kg/s, the pressure is 18.05 MPa, and the inlet water temperature is set as the design value of 335 °C.

3.2 Confirmation of reactor secondary circuit startup scheme

In this section, the mode of mass flow rate and temperature of the inlet water of the secondary circuit are

discussed and a more appropriate reactor startup scheme of the secondary circuit is selected. The calculation cases of different secondary circuit schemes are compared with the results calculated separately using the ATHLET system code. Before the calculation, it is necessary to set the judgment criteria to reach a steady state from the start of the reactor. The following judgment criteria are used. (1) The oscillation amplitude of the mass flow of the primary circuit around the design value is less than 1%. (2) The temperature oscillation range of the core outlet and inlet coolant is less than 0.1%. (3) The oscillation amplitude of the steam temperature at the outlet of the secondary side of the heat exchanger is less than 0.2%. When the above parameters all reach the judgment criteria, it is considered that the startup has reached a steady state.

3.2.1 The different modes of feedwater flow in the secondary circuit

In this section, it is assumed that the water temperature at the inlet of the secondary circuit is maintained at the design value and the mass flow rate of the water at the inlet of the secondary circuit is selected for studying the respective linear growth and step growth. The two growth modes are shown in Fig. 2a. The step amplitude of the step type is 10%. The two schemes reach the maximum mass flow rate at the same time point, that is, the time point corresponding to the increase in core power to 100%. The inlet water temperature of the secondary circuit is maintained at the design value of 335 °C during the entire reactor startup phase.

The temperature change of the core inlet coolant during the startup process is shown in Fig. 2b. As shown in the figure, compared with the linear growth, the step flow growth in the secondary circuit will cause a greater degree of the core inlet coolant temperature drop. The steam temperature at the outlet of the secondary circuit is shown in Fig. 2c. As depicted in the figure, the step-type growth of the secondary circuit will result in the oscillation of the water and steam temperature at the outlet of the secondary circuit in the initial stage of startup and is more severe, which is not conducive to the stable operation of the reactor.

By comparing the two types of feedwater flow of the secondary circuit, it can be found that a lower supercooling degree of the lower plenum, a more stable outlet steam temperature of the secondary circuit, and lower peak values of some parameters will appear when the feedwater flow of the secondary circuit increases linearly, which is more conducive to the safe and stable startup of the reactor. Therefore, the scheme with linear growth of feedwater flow in the secondary circuit is selected to carry out the subsequent analysis.

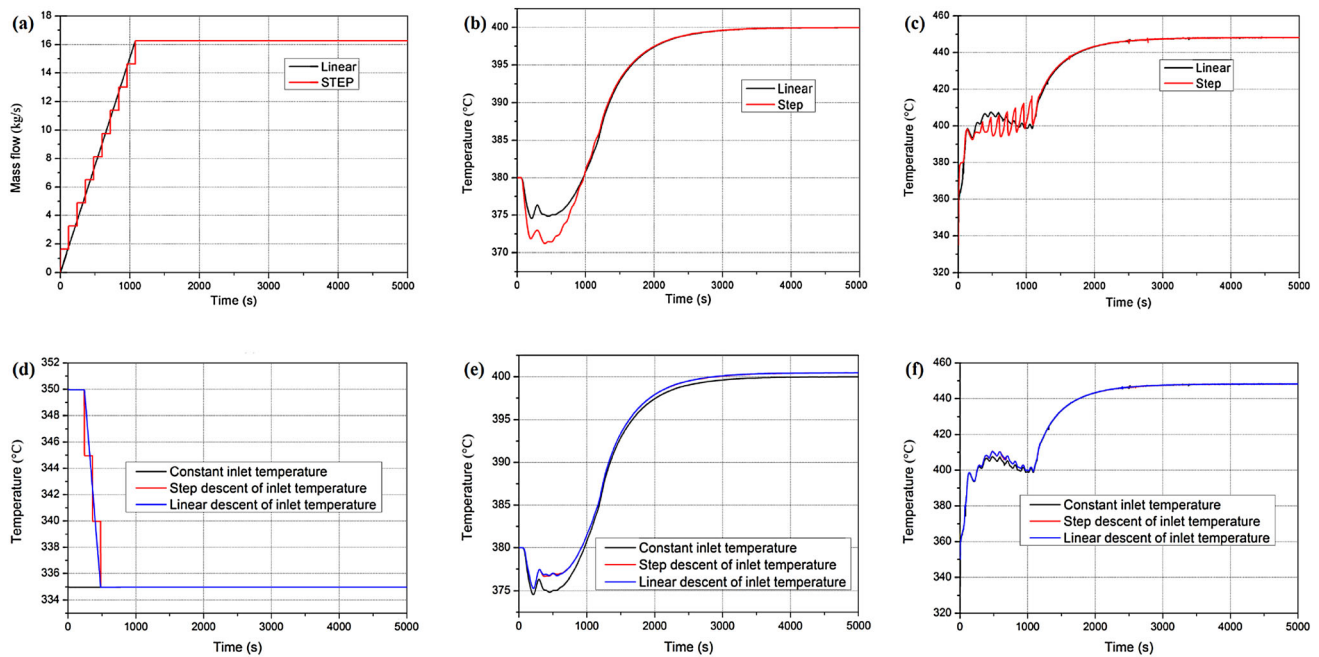


Fig. 2 (Color online) Determination of secondary circuit scheme

3.2.2 The different modes of inlet water temperatures in the secondary circuit

Based on the given linear growth of the inlet water flow of the secondary circuit, three different inlet water temperatures of the secondary circuit are selected. The three schemes are as follows: (1) the temperature is the design value of 335 °C, (2) the initial value is 350 °C and then decreases linearly, and (3) the initial value is 350 °C and then decreases step by step. The water temperature at the inlet of the secondary circuit is shown in Fig. 2d. The step-type feedwater temperature falls with the step of power growth with step amplitude of 5 °C. The temperature starts to decrease when the power is up to 20% of the full power for schemes 2 and 3. The temperature drop to the design value corresponds to a power of up to 40% of the full power.

The average temperature variation of the core inlet coolant during the startup process is shown in Fig. 2e. As can be observed in the figure, the temperature of the core inlet coolant in the final steady state of the reactor startup in the three calculation schemes is basically the same, reaching the design value of 400 °C. However, the coolant temperature at the core inlet will be lower in the initial stage of the reactor startup in scheme 1, which will lead to a higher degree of supercooling at the core inlet.

The outlet steam temperature of the secondary circuit is shown in Fig. 2f. It can be observed that the outlet steam temperature does not change by step type in the process of rising; however, there is a certain degree of oscillation

when the core power reaches between 40 and 80% of the full power. At this point, the outlet steam temperature of the secondary circuit in schemes 2 and 3 is higher than that in scheme 1.

By comparing the three different water temperature schemes, it is determined that the steam temperature at the secondary circuit outlet has almost the same variation trend. The changes in various parameters in schemes 2 and 3 are basically the same; however, the two schemes will reduce the degree of supercooling of the lower plenum coolant, which is more conducive to the safe startup of the reactor. In this study, a scheme with a step-type decline in water temperature at the inlet of the secondary circuit was selected as an example to carry out the subsequent analysis.

4 Study of SNCLFR-100 instability under different reactor startup schemes

Based on the selected startup scheme, different groups of startup schemes are added for comparison to determine a more appropriate primary circuit power-step amplitude and duration time. A total of five groups of schemes are listed in Table 1. In all the reactor startup schemes, the reactor is started in a cold startup process; that is, it starts from a power of zero. The total calculation time for all the schemes is 5000 s. The variation in power during the startup process is shown in Fig. 3a.

To evaluate the results of all the reactor startup schemes and the existing flow instability, the multi-scale coupling

Table 1 Different schemes for startup

Power-step amplitude (%)	Duration time (min)
5	2
10	2
20	2
10	1
10	5

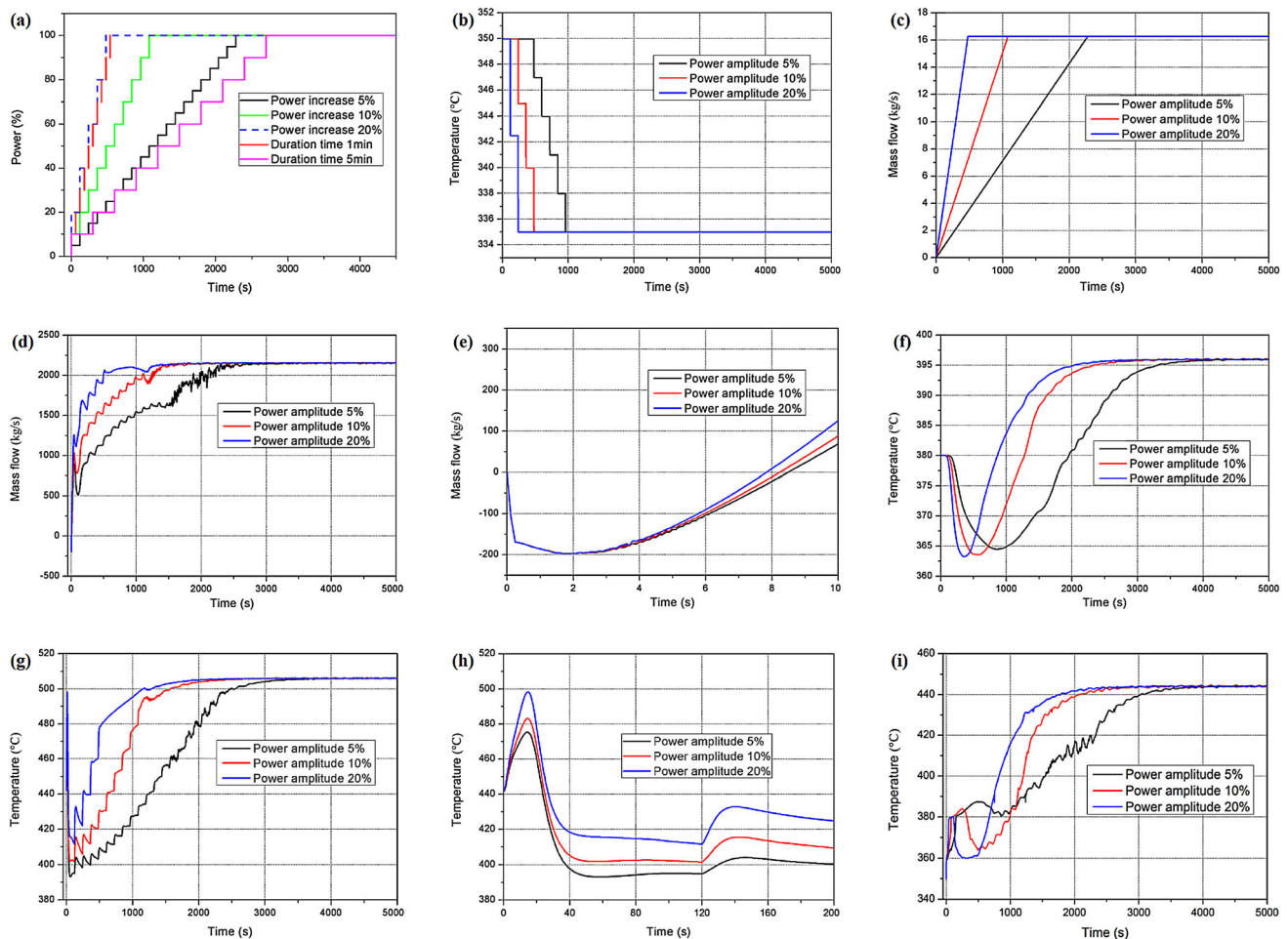
code ATHLET-OpenFOAM is used to complete all the calculations. The calculation results of all startup schemes are evaluated in terms of the following indicators:

- (1) Whether the maximum temperature of cladding exceeds the design value of 650 °C.
- (2) Time from zero to full power t_1 , time from initial time zero to final steady-state operation t_2 , and time from full power to steady-state operation ($t_2 - t_1$) in various reactor startup schemes.

- (3) Whether there is a backflow phenomenon in the core and the duration of backflow.
- (4) Frequency, amplitude, and time of flow oscillation in the primary circuit.
- (5) The degree of supercooling in the lower chamber.

4.1 Study of the effects of power-step amplitude

In this section, three reactor startup schemes with different power-step amplitudes are selected for calculation under the same power duration time, among which the three types of power-step amplitudes are 5%, 10%, and 20%, respectively, and the power duration time is 2 min. The temperature and mass flow rate of water at the inlet of the secondary side of the main heat exchanger are shown in Fig. 3b and c, respectively. As shown in Fig. 3c, the time point when the water temperature at the inlet of the secondary side of the heat exchanger of the three schemes begins to decrease is not consistent. This is because they all correspond to the time point when the power in each

**Fig. 3** (Color online) Effects of power-step amplitude

scheme rises to 20%. When the core power is at 40% of the full power, the water temperature at the inlet of the secondary side of the heat exchanger drops to the design value of 335 °C. As shown in Fig. 3c, the mass flow rate of the feedwater at the inlet of the secondary side of the heat exchanger increases linearly and the mass flow rate reaches the design value when the core power reaches 100% full power.

Figure 3d and e shows the variation in the total core mass flow rate in the three reactor startup schemes with different power-step amplitudes. It can be observed in the figure that the backflow appears in the reactor core and the maximum mass flow rates of the backflow are almost the same. When the mass flow rate approaches the maximum value of the design, the vibration frequency and amplitude begin to increase, and the smaller the power-step amplitude is, the higher the vibration frequency is, the larger the amplitude and the longer the oscillation duration time is. The larger the power-step amplitude, the shorter the backflow duration time, because the larger the power-step amplitude, the higher the cladding temperature in the same time in the initial stage of startup and the higher the coolant temperature in the fuel assembly area. The greater the coolant temperature difference between the inner fuel assembly area and the upper plenum, resulting in a larger density difference and eventually a larger driving pressure head. Therefore, the mass flow rate in the core quickly returns to a positive value.

As shown in Fig. 3f, there is no obvious difference in the supercooling degree of the lower plenum among the three schemes. When the core power reaches more than 50%, the supercooling of the lower plenum will be improved; that is, the core inlet coolant temperature will start to rise rapidly.

Figure 3g and h shows the maximum cladding temperatures of the three different schemes. According to the figures, the maximum peak temperatures of the cladding in the three schemes are all within the limit value. The larger the power-step amplitude is, the larger the peak temperature is; the smaller the drop after the peak temperature is, the higher the vibration range is.

Figure 3i shows the temperature of the water and steam at the outlet of the secondary side of the heat exchanger in the three different schemes. It can be observed from the figure that the larger the power-step amplitude is, the more obvious the peak value of the steam temperature at the outlet is at the early stage of startup and the faster it reaches the peak value.

When the total mass flow rate of the reactor core, the steam temperature at the outlet of the secondary side of the heat exchanger, and the coolant temperature at the inlet of the reactor core reaches the steady state, the entire reactor can be considered to have reached the steady-state

operation from the reactor startup. Taken together with the three variables, the time for the three different startup schemes to reach a steady state is shown in Table 2. Moreover, t_1 , t_2 , and $(t_2 - t_1)$, respectively, represent the time for the core to reach full power, the time for the reactor to reach steady state from startup, and the time for the reactor from full power to reach a steady state.

As can be observed in Table 2, the larger the power-step amplitude is, the shorter is the total time taken by the reactor from startup to full power and steady-state operation. Meanwhile, the longer is the time from reaching full power to the steady-state operation, the smaller is the power-step amplitude and the faster the startup process stabilizes.

The above three schemes of different step amplitudes are compared in terms of larger or smaller power-step amplitude. The larger the power-step amplitude, the longer the time is from full power to the steady state, the higher are the coolant flow rate and temperature, and the greater is the degree of supercooling in the lower plenum, which is not conducive to startup, especially after adding the reactivity feedback. However, the shorter is the duration time of the core backflow, which is more conducive to the establishment of natural circulation, the smaller is the frequency and amplitude of the later flow oscillation and the shorter is the oscillation duration time.

In summary, larger power-step amplitude and smaller power-step amplitude have opposing advantages and disadvantages. According to the comprehensive evaluation index, a compromise power-step range of 10% is selected as the optimal scheme.

4.2 Study on the effects of power duration time

In this section, three reactor startup schemes with different power duration times are selected for the calculation under the same power-step amplitude. The three power duration times are 1 min, 2 min, and 5 min, respectively, and the power-step amplitude is 10%. The water temperature and mass flow rate at the inlet of the secondary side of the reactor main heat exchanger are shown in Fig. 4a and b, respectively. The water temperature at the inlet of the secondary side of the heat exchanger remains at 350 °C

Table 2 Steady-state time of startup schemes with different power-step amplitudes

Power-step amplitude (%)	t_1 (s)	t_2 (s)	$(t_2 - t_1)$ (s)
5	2280.0	3625.2	1345.2
10	1080.0	2708.7	1628.7
20	480.0	2612.0	2132.0

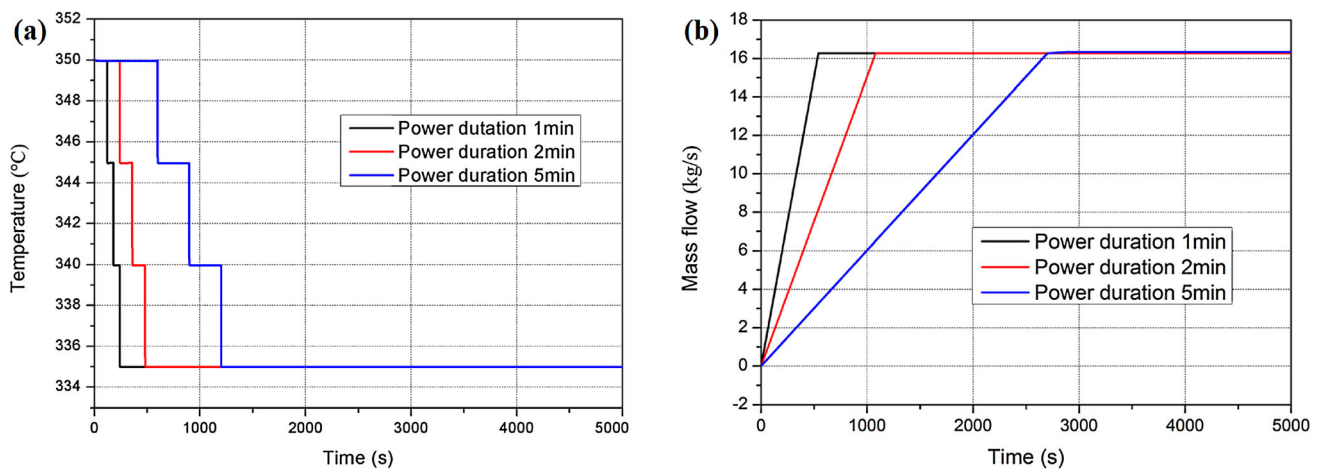


Fig. 4 (Color online) Temperature and mass flow rate of water at the inlet of the secondary side of heat exchanger

during the initial startup stage and begins to decline until the end of the stage when the reactor core is 20% of full power. In the three reactor startup schemes, the temperature drop gradient is 5 °C and the inlet water temperature drops to the design value of 335 °C just after the stage when the core is at 40% full power.

The total mass flow of the reactor core in the three reactor startup schemes with different power duration times is shown in Fig. 5a and b. As can be observed from the figures, the core has a certain degree of backflow. The peak mass flow rate of the backflow is almost the same for all three schemes. The longer the power duration time is, the lower the flow oscillation frequency will be in the first half stage before approaching the steady state. At this stage, the

power does not reach the design value and the mass flow rate oscillates with the power change. The increase in power increases the temperature difference between the fuel assembly and the coolant, leading to a greater density difference and driving head, thereby increasing the flow rate. The longer the power duration is, the slower the power increase is and the lower is the flow oscillation frequency.

Figure 5c shows the change in the core inlet coolant temperature during reactor startup with three different schemes. As can be observed from the figure, in the scheme with a power duration time of 5 min, the lowest peak temperature of the coolant temperature is 368.5 °C, which is significantly higher than that of the other two schemes and will help slow the supercooling of the lower

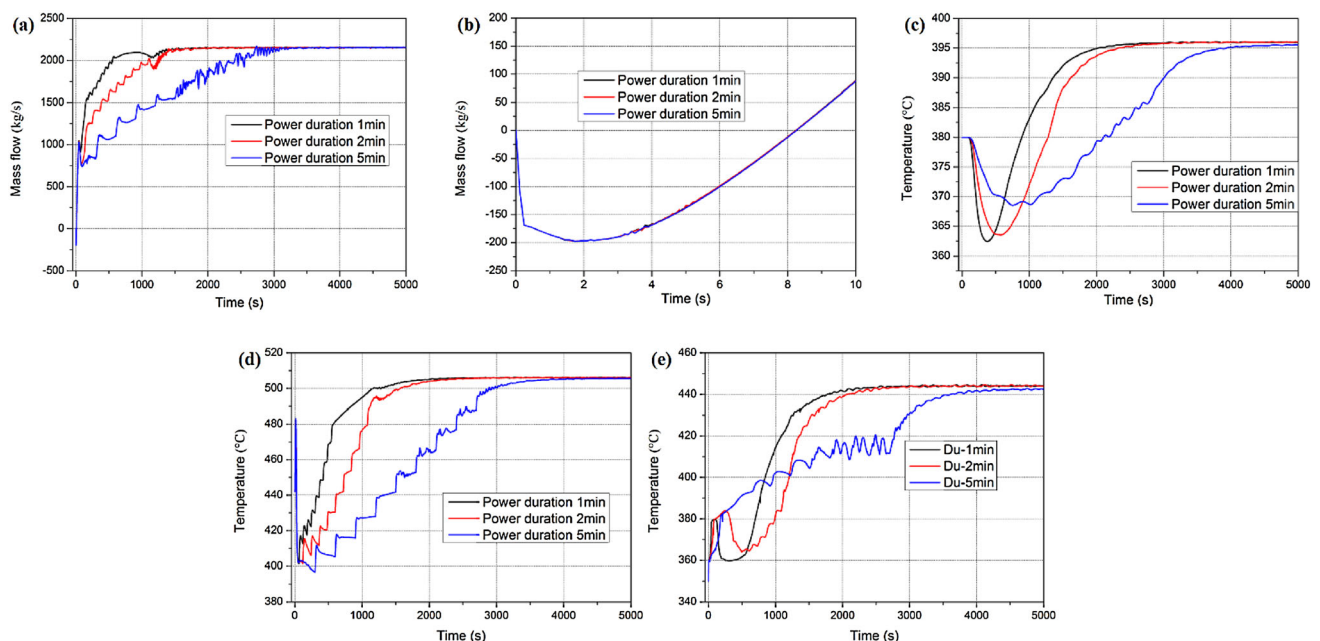


Fig. 5 (Color online) Effects of power duration

plenum. As the power continues to increase and the coolant temperature at the core outlet continues to rise, the coolant temperature at the core inlet begins to rise. Moreover, the longer is the power duration time, the slower is the rise. This is because the longer is the power duration, the slower is the power rise.

Figure 5d shows the variation in the maximum cladding temperature during startup. It is evident from the figure that the peak values of the cladding temperature in the three schemes with different power durations are almost the same at approximately 483.1 °C and the final stable values are all less than 510 °C, which is within the safety limit of cladding. In the process of increasing the cladding temperature, there will be a step rise similar to power, which directly leads to the same rising trend of mass flow rate.

Figure 5e shows the temperature changes of the water vapor at the outlet of the secondary side of the heat exchanger in three different startup schemes. It is observed in the figure that the longer the power duration time is, the more stable is the temperature of the water vapor at the outlet of the secondary side of the heat exchanger. It will rise at the initial stage of startup; however, the temperature oscillates greatly in the period before the power is close to full power.

Similarly, the corresponding steady-state times of the three different startup schemes are listed in Table 3. It is shown in the table that the longer the power-step duration time is, the longer is the total time taken by the reactor from startup to steady-state operation. However, the shorter the time is from reaching full power to steady-state operation—indicating that the power duration time is longer—the faster it stabilizes in the startup process.

The above three schemes with different power duration times, coolant flow rates, and coolant temperatures are compared with the peak temperature of the cladding in the three schemes being all the same and the duration of core backflow being almost the same. The longer the power duration time is, the shorter the stable time is from full power to the final steady state. Although the flow oscillation amplitude in the scheme with a power duration time of 5 min is slightly larger and the oscillation duration time is longer, the flow oscillation frequency is significantly lower

and the degree of supercooling of the lower plenum is also significantly improved.

In summary, although a longer power duration time and a shorter power duration time each have advantages and disadvantages, the longer power duration time scheme has more significant advantages. Therefore, a power duration of 5 min is the optimal scheme.

5 Conclusion

In this paper, the startup process and the key focus areas of natural circulation lead-cold fast reactors were briefly described. The startup schemes of natural circulation boiling water reactors, sodium-cold fast reactors, and driven lead-cold fast reactors were referenced. Through research and comparison, a comprehensive startup scheme for a small natural circulation lead-cold fast reactor SNCLFR-100 was determined. The criteria for achieving a steady state were given. The main contents and conclusions are as follows.

- (1) The power in the primary circuit increases as a step function based on the existing reactor types. A secondary circuit scheme was determined in which the mass flow rate at the inlet of the secondary side of the heat exchanger increases linearly and the inlet water temperature decreases step by step.
- (2) Based on the comprehensive reactor startup scheme determined above, the reactor startup schemes with different power-step amplitudes were compared. Under the premise of the same power duration time of 2 min, three reactor startup schemes with power-step amplitudes of 5%, 10%, and 20% were selected for calculation and comparative analysis. According to the comprehensive evaluation index, the comprehensive scheme with power-step amplitude of 10% was the optimal scheme.
- (3) Under the premise of the same power-step amplitude of 10%, the three schemes of power duration times of 1 min, 2 min, and 5 min were selected for calculation and comparative analysis. According to the comprehensive evaluation index, the scheme with a power retention time of 5 min was the optimal scheme.

Table 3 Steady-state time of startup schemes with different power durations

Power duration (min)	t_1 (s)	t_2 (s)	$(t_2 - t_1)$ (s)
1	540	2517.8	1977.8
2	1080	2708.7	1628.7
5	2700	3953.5	1253.5

Acknowledgements Thank GRS for providing the ATHLET-Open-FOAM coupling code.

Author contributions All authors contributed to the study conception and design. Material preparation, data collection, and analysis were performed by Wen-Shun Duan, Ze-Ren Zou, Xiao Luo, and Hong-Li Chen. The first draft of the manuscript was written by Wen-

Shun Duan, and all authors commented on previous versions of the manuscript. All authors read and approved the final manuscript.

References

1. S.P. Wang, B.W. Yang, Effects of ocean motions on density wave oscillations under natural circulation. *Ann. Nucl. Eng.* **131**, 185–195 (2019). <https://doi.org/10.1016/j.anucene.2019.03.044>
2. S.P. Lakshmanan, M. Pandey, P.P. Kumar et al., Study of startup transients and power ramping of natural circulation boiling systems. *Nucl. Eng. Des.* **239**(6), 1076–1083 (2009). <https://doi.org/10.1016/j.nucengdes.2009.01.002>
3. P.K. Vijayan, H. Austregesilo, V. Teschendorff, Simulation of the unstable oscillatory behavior of single-phase natural circulation with repetitive flow reversals in a rectangular loop using the computer code ATHLET. *Nucl. Eng. Des.* **155**(3), 623–641 (1995). [https://doi.org/10.1016/0029-5493\(94\)00972-2](https://doi.org/10.1016/0029-5493(94)00972-2)
4. A. Satoh, K. Okamoto, H. Madarame, Instability of single-phase natural circulation under double loop system. *Chaos Solit Fract.* **9**(9), 1575–1585 (1998). [https://doi.org/10.1016/S0960-0779\(97\)00117-3](https://doi.org/10.1016/S0960-0779(97)00117-3)
5. S.Y. Jiang, M.S. Yao, J.H. Bo et al., Experimental simulation study on start-up of the 5 MW nuclear heating reactor. *Nucl. Eng. Des.* **158**(1), 111–123 (1995). [https://doi.org/10.1016/0029-5493\(95\)01020-I](https://doi.org/10.1016/0029-5493(95)01020-I)
6. K.L. Chen, C.Q. Yan, G.M. Fan et al., Experimental study on startup characteristics of passive residual heat removal system in molten salt reactor, in *Proceedings of the 15th National Conference on Reactive Thermal Fluid and the Annual Conference of the Key Laboratory of Thermal Hydraulic Technology of CNNC Nuclear reactor*, Shangdong (China), 2017
7. J. Gourdon, B. Mesnage, J. Voiteiller et al., An overview of Superphenix commissioning tests. *Nucl. Sci. Eng.* **106**(1), 1–10 (1990)
8. L. Luzzi, R. Ponciroli, S. Lorenzi et al., Petri Net approach for a Lead-cooled Fast Reactor startup design, in *Proceedings of the International Conference on Fast Reactors & Related Fuel Cycles: Safe Technologies & Sustainable Scenarios*, 2013
9. N. Wang, Study on natural cycle characteristics of fully natural cycle lead based fast reactor in reactor startup condition. Dissertation, Sun Yat-sen University, 2020 <https://thesis.sysu.edu.cn/paper-detail.html?paperId=147480>
10. D. Grishchenko, A. Papukchiev, C. Liu et al., TALL-3D open and blind benchmark on natural circulation instability. *Nucl. Eng. Des.* **358**(1), 110386 (2020). <https://doi.org/10.1016/j.nucengdes.2019.110386>
11. B. Deng, Y. Cui, J.G. Chen et al., Core and blanket thermal-hydraulic analysis of a molten salt fast reactor based on coupling of OpenMC and OpenFOAM. *Nucl. Sci. Tech.* **31**(9), 85 (2020). <https://doi.org/10.1007/s41365-020-00803-9>
12. J. Herb, Coupling OpenFOAM with thermo-hydraulic simulation code ATHLET, in *Proceedings of the 9th OpenFOAM Workshop*, Zagreb (Croatia), 2014
13. H.L. Chen, Z. Chen, C. Chen et al., Conceptual design of a small modular natural circulation lead cooled fast reactor SNCLFR-100. *Int. J. Hydrogen Energ.* **41**(17), 7158–7168 (2016). <https://doi.org/10.1016/j.ijhydene.2016.01.101>
14. K.L. Shi, S.Z. Li, X.L. Zhang et al., Partial flow blockage analysis of the hottest fuel assembly in SNCLFR-100 reactor core. *Nucl. Sci. Tech.* **29**(1), 16 (2018). <https://doi.org/10.1007/s41365-017-0351-3>